Accumulated Photon Echo in Er-Doped Fibers

Valéria L. da Silva* and Yaron Silberberg†
Bellcore, 331 Newman Springs Road,
Red Bank, NJ 07701, USA

Received March 20, 1995

Accumulated photon-echo experiments in Er-doped fibers with femtosecond and picosecond pulses are described. We explore the potential applications in ultrafast optical signal processing and demonstrate the advantages of a fiber-based system for studies of photon-echoes. A frequency domain model description of photon echo that is very suitable to describe photon-echo in doped-fibers is presented. Finally, we report an experiment using a nonlinear pulse shaper that mimics the physics of accumulated photon echo process in an inhomogeneous absorber, with the difference that echoes are generated both preceding and following the excitation pulses. The causality of both processes is discussed.

I. Introduction

Optical fibers have proved to be an attractive medium for studies of many optical nonlinear effects[1]. In most case, the nonlinearity exploited was the Kerr effect in silica-based fibers. The recent development of fibers doped with rare-earth ions now allows the study of resonant nonlinear interactions. Coherent effects, in particular, become important for pulses that are shorter than or comparable to the dephasing time of the impurity ions in the fiber. In fact, it has been recently reported the observation of photon echo in Nd-doped and Er-doped fibers[2−5] and self-induced transparency in Er-doped fibers[6]. In this paper, we review a number of experiments where photon-echo in Er-doped fiber is investigated and demonstrate its potential application in ultrafast optical signal processing. We also present a frequency domain model of the photon-echo phenomena which is also valid in the strong saturation regime. This model makes clear the similarities between photon-echo, spectral hole-burning and Fourier holography, which helped us design an experiment where "non-causal" echoes can be observed[7].

Photon-echoes are obtained in an inhomogeneously broadened two-level system. Fig. 1 shows the three most common photon-echo techniques. To obtain echoes, both the pulse duration t_p and the separation τ between the excitation pulses must be of the order of the homogeneous dephasing time T_2 or shorter. In the original two-pulse photon-echo scheme shown in Fig. 1(a) [8], the optical pulses should have areas of $\pi/2$ and π in order to maximize the echo generation. In an stimulated, or three-pulse, echo experiment (Fig. 1(b)) [9], a third pulse that arrives at a delay T after the original pulse pair will stimulate an echo. The delay T could be much longer than the dephasing time length, but it should be shorter than the radiative lifetime T_1. An accumulated photon-echo experiment (Fig. 1 (c)) resembles the standard two pulse experiment, however the excitation is repeated many times within the radiative lifetime. This results in great enhancement in the efficiency of the generated echo[10−12].

The accumulated photon-echo process is perfectly phase-matched only when the two excitation pulses are collinear, either co- or counter-propagating as in Fig. 2(a). However, many experiments in bulk media are performed with a small angle between the two pulses (fig.2(b)). In this case, the echoes can be spatially separated from the excitation pulses, facilitating its detection. Obviously, our experiments in fibers must be collinear, and therefore must be time resolved to observe echoes.

*Present address: Corning Inc., Corning, NY 14831, USA
†Present address: Dept. of Physics of Complex Systems, Weizmann Institute of Science, Rehovot 76100, Israel

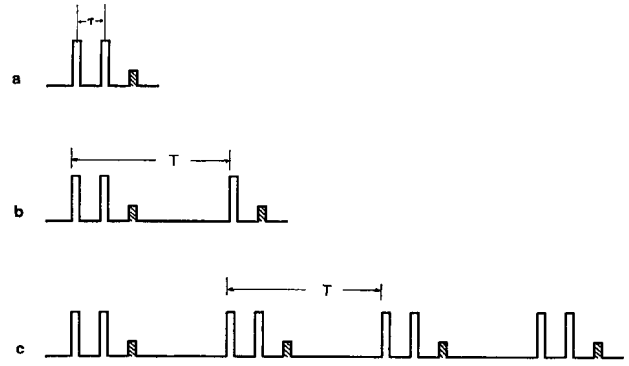

Figure 1. Photon-Echo experiments. (a) Two-pulse echo. (b) Stimulated photon echo. (c) Accumulated photon echo.

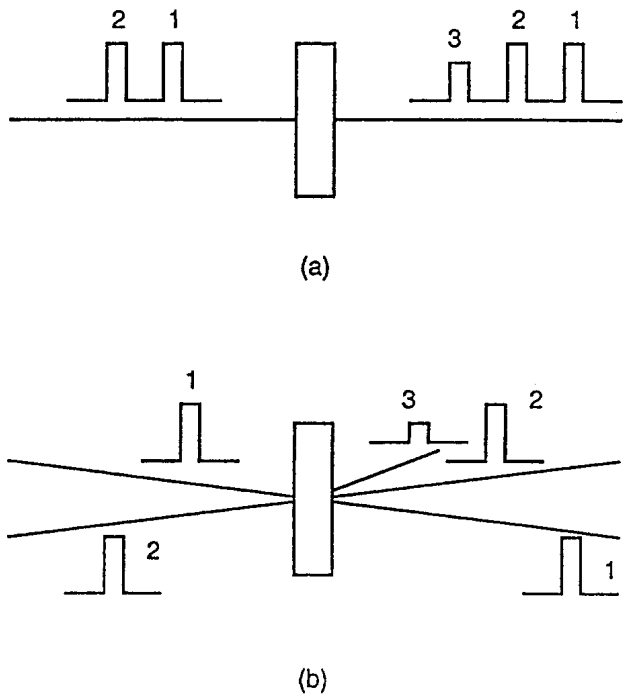

Figure 2. Experimental geometries for photon-echo. (a) Collinear arrangement for exact phase matching, (b) noncollinear arrangement, in which the echo is emitted in a different direction.

II. Frequency-Domain Model

The most common approach to the analysis of accumulated photon-echo processes is a time- domain analysis[11,12], which usually involves approximations that result in expressions that are equivalent to third-order ($\chi^{(3)}$) expansion in the input field. These theories are not sufficiently accurate to describe the interaction in a fiber, where significant saturation of the transition may occur. Moreover, the time-domain picture, which is very intuitive in a simple echo experiment with $\pi/2$ an π excitation pulses[8], loses much of its simplicity when stimulated and accumulated echo are considered. Recently, we have shown that a frequency domain model of the photon-echo interaction is particularly suitable for doped fibers. It can describe the accumulated photon-echo in a simple and intuitive way and analyze the optically dense, highly saturated absorption in a doped fiber[5].

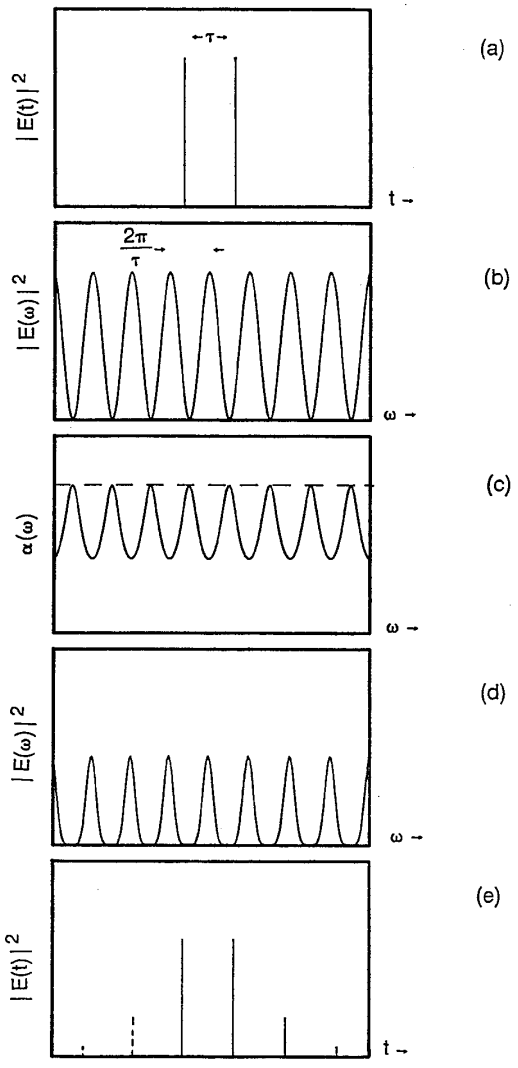

Figure 3. The spectral domain view of photon-echo in an ideal experiment with narrow input pulses and extreme inhomogeneous line: (a) the input pulses in the time domain, (b) the input pulses in the frequency domain, (c) the saturated frequency grating in the absorption spectrum, (d) the transmitted spectrum, and (e) the time domain temporal signal showing the echoes. The broken lines are noncausal echoes that are canceled through the interference of amplitude an phase gratings of the transmission function.

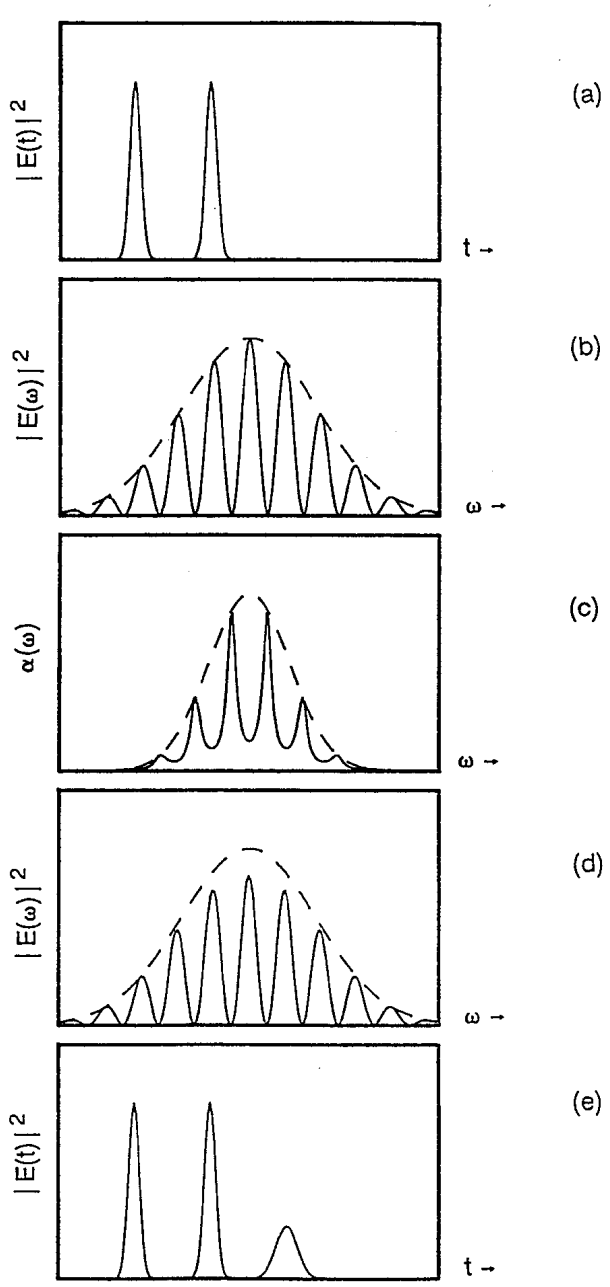

Figure 4. The frequency domain view of photon echo, same as Fig. 3 with finite duration for the input pulses and finite width inhomogeneous absorber. The echo pulse is longer than the input pulses because of the narrow inhomogeneous absorption line.

The main ideas are summarized in Figs. 3 and 4. A full description of the frequency-domain model is reported in [5]. Fig. 3 shows an idealized situation, with infinitely short excitation pulses and infinitely broad inhomogeneous absorber. First, we note that two excitation pulses separated by τ (Fig. 3(a)) are characterized by a sinusoidally modulated spectrum (Fig. 3(b)). This spectrum irradiates the inhomogeneous line and saturates a population grating, which results in a modulated absorption and index gratings (only the absorption is shown in Fig. 3(c)). The transmitted light is affected by these gratings; its spectrum is still periodic but no longer sinusoidal (Fig. 3(d)). In the time domain, this means that higher harmonics, or echoes, have been generated (Fig. 3(e)). The amplitude and phase transformation of the spectrum must be causal, i.e., echoes are generated only following the excitation pulses. Note that this picture is a precise Fourier transform of a wave mixing process in a saturable absorber. By transforming $t \leftrightarrow \omega$ in Fig. 3 we get the time domain description of a wave mixing process, with the important difference that the wave mixing will generate harmonics on both sides of the two input frequencies, because there is no causal restriction on the variable ω.

In Fig. 4 we repeat the model of Fig. 3 for more realistic finite duration input pulses and absorption width. In this example, the input pulses are shorter than the inhomogeneous dephasing time, hence their spectra are wider than the absorption line spectrum. Qualitatively, the process remains unchanged. This frequency-domain model can easily explain a number of phenomena:

1. The grating saturated in the absorption spectrum decays with the characteristic T_1 time constant, which could be much longer than the coherent dephasing time T_2. Therefore any additional pulse sent through the medium before the grating has decayed will get modulated by the transmission function and exhibit side bands - echoes- in the time domain. This is the basis for the stimulated echo process (Fig. 1(b)).

2. The long lifetime of the saturated frequency grating is also the reason for the increased efficiency of the accumulated echo: The grating is saturated by the accumulated effect of many pulse pairs, integrated over the T_1 lifetime.

3. As the time delay τ between the pulses is increased, the grating becomes denser, and eventually it is limited by the fine features into the absorption spectrum. This causes the decrease in the efficiency of the echo generational which is the basis for measurements of homogeneous coherent

lifetimes.

4. The same model can be used to describe the photon-echo in a gain medium. Note, however, that the transmission functions in a medium with saturable gain and absorption are out of phase. As a consequence, the echoes generated in both situations will also be out of phase.

We finally note that the process described here, which involves recording of a diffraction from spectral gratings closely resembles an holographic process. Indeed, several groups have considered the similar process of spectral hole burning for time-domain holography[13].

III. Experiment

Erbium-doped fibers are particularly important in optical communications because the ${}^4I_{15/2}-{}^4I_{13/2}$ transition at 1.53 μm coincides with the minimum loss region of silica fibers. These fibers can be pumped by diode lasers and have been used as amplifiers and as lasers in the 1.53 μm region[14,15]. The radiative lifetime of the upper level is $\sim$10 ms. Both levels are Stark-split into a manifold of sublevels, which result in a broad absorption and fluorescence spectra with homogeneous line characteristics, with $T_2 \approx 100$ fs at room temperature. At low temperatures, however, the dephasing time increases from $T_2 \approx 100$ fs to $T_2 \approx 1$ ns at 4.2 °K, and the transition becomes inhomogeneously broadened. At this low temperature, only the lowest stark sublevels are populated and the inhomogeneous width of the transition is about 10 nm [14].

The fiber used had a silica cladding and an Er-doped germanium-calcium-aluminum silicate core[16] with a diameter of 4 μm. The peak absorption was measured to be 10 dB/m at 1.53 μm at room temperature. A section of this fiber was coiled to a 4 cm diameter, spliced to dispersion-shifted pigtails and immersed in liquid helium. Note that by using a fiber system, we eliminate the need for windows, vacuum and other difficulties associated with cryogenic optical systems.

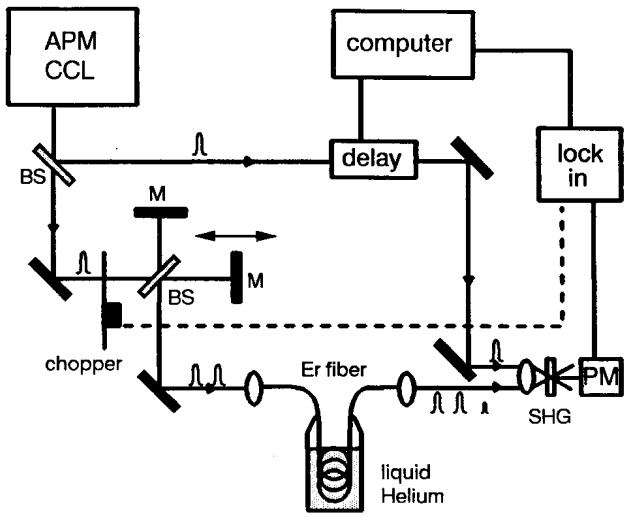

Figure 5. The experimental setup for observation of femtosecond accumulated photon echoes. APM CCL - additive-pulse-mode-locked color center laser, BS- beam splitters, M- mirrors, PM - photomultiplier.

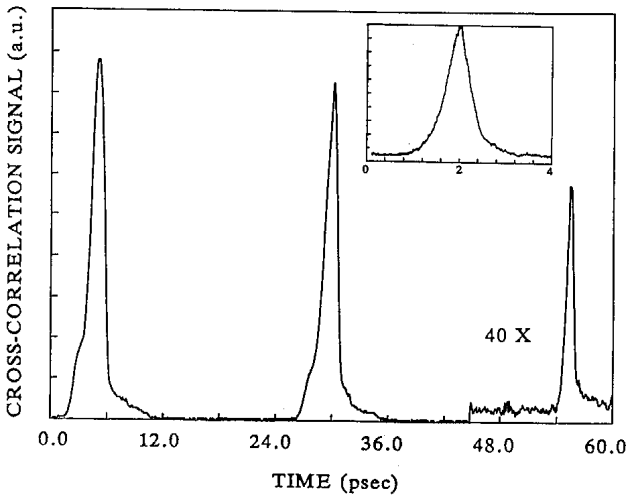

Figure 6. Cross-correlation trace showing the two excitation pulses and the first order echo generated in a 4.5 m erbium-doped fiber. The input pulse separation is 25 ps. Inset: The shape of the time-resolved echo in a 3 m fiber section, showing a 580 fs FWHM echo pulse.

The basic experimental setup is shown in Fig. 5. An NaCL:OH^- color center laser with additive-pulse mode-locking[17] was used as the optical pulse source. The pulses produced by the laser were less than 200 fs long and they were centered at 1.53 μm. The laser pulse repetition rate is 82 MHz while the Er^{3+} relaxation time T_1 is 10 ms. Therefore approximately 10^6 pulse pairs were coupled into the fiber within T_1. A Michelson interferometer was used to generate a pulse pair with controllable delay. These pulses could be coupled to the

fiber with a maximum average power of about 4 mW. The output from the tested fiber was time-resolved by cross-correlating it with a delayed pulse of the laser.

Fig. 6 shows the cross-correlation trace of the output signal emerging from the fiber with a short pulse, when the two input pulses are separated by 25 ps. A 4.5 m section of cooled erbium fiber was used in this experiment. As expected, an echo is observed 25 ps after the second pulse. Note also the free-induction decay emission that follows each of the pump pulses. The echo pulse duration from the 4.5 m fiber was about 800 fs. It is likely that this pulse is broadened by the dispersion in the fiber, estimated to be about 10 ps/Km.nm. A 3.0 m section of doped fiber generated a shorter echo of about 580 fs, as shown in the inset of Fig. 6. The echo duration was measured to be only 500 fs in a 0.8 m long fiber, where dispersion effects should be minimal.

Assuming an inhomogeneous line shape $g(\omega) \propto \exp[-(\omega - \omega_0)^2 T_2^{*2}]$ with a FWHM of $\Delta\omega_{\text{in}} = 2\sqrt{\ln 2}/T_2^*$, the FWHM echo pulse duration for short excitation pulses is $T^{\text{echo}} = 2\sqrt{2\ln 2}T_2^*$ [5]. Expressed in wavelength terms, the echo duration is

$$T^{\text{echo}} = \frac{2\sqrt{2}\ln 2}{\pi}\frac{\lambda^2}{c\Delta\lambda} \qquad (1)$$

A 10 nm linewidth then yields a 490 fs echo, in good agreement with our experiment. Although we did not measure the value of homogeneous lifetime T_2 in our fiber, we could not detect a significant drop in the echo intensity even for pulse separations of 200 ps , which suggests that T_2 is much longer than that. The echo intensity in the 4.5 m long fiber was about 50 times weaker than the transmitted excitation pulses. This ratio was about 100 in the 3 m fiber. The echo was considerably weaker in a 0.8 m long fiber. This suggests that the echo is generated along the entire fiber length. Note again that this is an accumulated echo experiment, and although each of the individual pulses' area is much smaller than π, the absorption is strongly saturated by the accumulation of many pulses during T_1.

One advantage of this experimental setup is that an erbium diode amplifier can be used to amplify the input pulses before they entered the cooled fiber, in order to study the process at even higher powers. We used a 10 m long amplifier, made from the same fiber, that was pumped by a second color-center laser at a wavelength of 1.48 μm. In addition to amplifying the pulses, the erbium-doped amplifier ensured that they are spectrally matched to the erbium transition, and since the amplifier was highly saturated it helped to stabilize the power of the injected signal. We found it helpful to spectrally filter the signal before coupling it to the amplifier. This was accomplished by using a grating and lens system, similar to that used for pulse shaping[18], and by placing an aperture at the focal plane where the spectrum is dispersed in space. This filtering eliminated a strong narrow line that was produced by our mode-locked laser. It also broadened the pulses to about 1 ps. These longer pulses were better matched to the amplifier peak gain as well as to the peak absorption of the cooled fiber. The amplified signal had about 10 mW average power; with this power the absorption could be saturated from 45 dB to less than 5 dB. Even though the area of each individual pulse is smaller than $\pi/20$, we could observe up to three orders of echoes, as can be seen in Fig. 7.

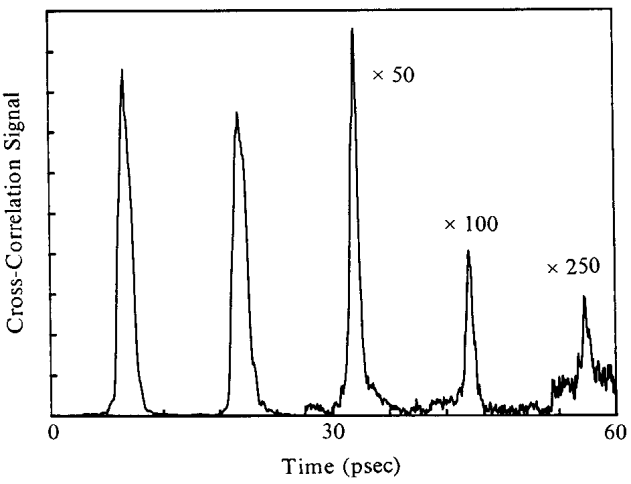

Figure 7. Cross-correlation trace showing three orders of echoes.

Photon-echo experiments in fibers can be significantly different from experiments in bulk media because the absorption can be easily saturated in the fiber. That allows the use of fiber lengths that are long compared with the absorption length, where propagation effects become important. This is a regime that is not easily accessible in bulk media. For example, we discovered that the second echo pulse shows a peculiar behavior: it has a double-peaked shape for some input

powers. This is the result of the interference between two echoes that are generated through different mechanisms and it is a consequence of using an optically thick medium. A detailed description of this phenomena can be found in [5].

Another advantage of the fiber geometry is the ease with which the system can be inverted. In fact, we recently reported photon-echo experiments with Er-doped fiber *amplifiers*[4]. To our knowledge, this was the first demonstration of photon-echo in any inverted medium.

IV. Signal Processing in Fibers

Photon-echo techniques have been proposed as a basis for time-domain optical memories[19] and ultrafast signal processing[20], and several demonstrations have been reported in gases and bulk organic and inorganic solids at cryogenic temperatures[20,21]. In such applications, the longest signal that can be recorded is of the order of the homogeneous lifetime T_2, the time resolution is the inhomogeneous lifetime T_2^*, and the storage time is the radiative lifetime T_1. The ${}^4I_{13/2} - {}^4 I_{15/2}$ transition of erbium in aluminosilicate fibers centered at 1.53 μm is strongly inhomogeneously broadened at 4.2 °K [14]. The use of Er-doped fibers for these applications offer a major advantage in terms of significant simplification of alignment and cooling requirements, as well as compatibility with many highly developed fiber based components.

Optical storage using photon-echo is one of the simpler schemes for time-domain processing of optical pulses using photon-echo and it was first suggested by Mossberg[19]. In this configuration, the echo is recorded between an information-containing data pulse (possibly a sequence of pulses) and a single write pulse. A third pulse, the read pulse, is used to recall the stored information by stimulating an echo. More complicated signal processing operations, such as time reversal and convolutions, are also possible. To understand the basis for all these applications, consider Fig. 8, which describe a Fourier holography setup[22]. In the case where point sources are used (Fig. 8 (a)), the experiment is completely analogous to the photon-echo process of Fig. 3. The Fourier lens transform the point sources to plane waves, which record a grating in the recording medium. The input wave can diffract from this grating to reconstruct each other or to generate higher orders of diffractions, the equivalent of echoes. Of course, in this scheme there are no causal limitations, and higher orders are generated symmetrically on both sides of the input.

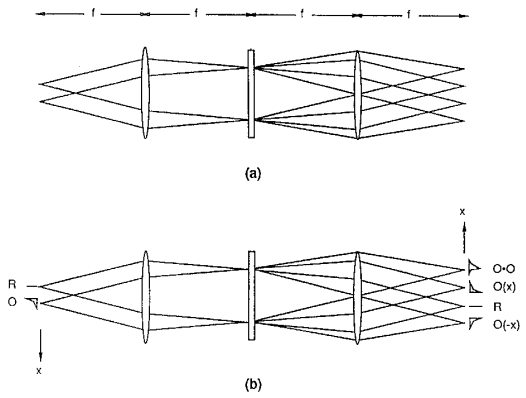

Figure 8. In Fourier-Holography lenses transform the input and output fields onto the recording medium. (a) With point source excitation Fourier holography is analogous to the photon-echo process as depicted in Fig. 2. A sinusoidal grating in the recording medium generates new diffraction orders at the output plane. (b) In signal processing applications, an interference of an object (O) and reference (R) waves is recorded, and then used to convolve these or other field with the object. With point-source reference waveform as shown, signal reversal and autoconvolution are obtained at higher orders.

Fourier holography can be used in signal processing when one (or both) of the input patterns carry information, as in Fig. 8 (b). In this case the grating in the Fourier plane is not sinusoidal, but it encodes the phase and amplitude information of the object wave. The hologram can now be used to reconstruct the object wave, or to generate more complex fields in the higher diffracted orders[22]. In view of this analogy, photon echo may be thought of as time domain holography. This analogy has been pursued by several research groups to reconstruct and manipulate temporal fields[13,21].

Although in our experiment the echo is generated through the accumulating effect of many pulses, we can still demonstrate the correlation between the shapes of the echo and the excitation pulses, which provides the basis for these signal processing applications. For this purpose, we substituted one of the excitation pulses by a double-peaked pulse, which serves the role of the object wave. This double pulse, with 3 ps separation, was

obtained by exploiting the birefringence of a 10 mm long KTP crystal, which was introduced into one of the arms of the interferometer. The relative intensity of the two peaks was adjusted by rotating the crystal. A polarizer was inserted before the fiber in order to assure that both excitation pulses were linearly polarized in the same direction. An Er-doped fiber amplifier was used in this experiment to amplify the input pulses before they enter the fiber under test, in order to enhance the generated echo.

Fig. 9(a) shows the echo generated when the double-pulse is the first to enter the fiber. Ideally, the echo in this case should be a time-reversed replica of the first excitation pulse. Time-reversal is clearly demonstrated, although it is also evident that the ratio of the two peaks is distorted. Fig. 9 (b) shows a similar experiment where the double pulse was arriving second. The echo clearly shows a triple peaked signal; in the small signal limit, this echo can be shown to be the autoconvolution of the second excitation pulse. Again, we observe significant distortion of the resulting pulse shape, particularly when the excitation intensity was increased. The distortions are the result of coherent coupling effects in the strongly saturated system. In order to reproduce undistorted signals the small signal absorption should be kept low, with $\alpha_0 L < 1$.

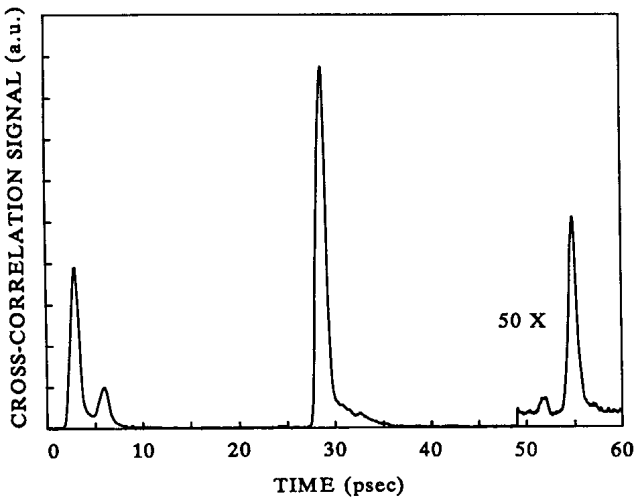

Figure 9. Demonstration of (a) time-reversal and (b) autoconvolution with picosecond signals. The object wave in both cases is a pulse doublet.

V. Noncausal photon-echo

In the photon-echo process described before, the excitation pulse pair saturates a frequency grating in the inhomogeneous line. There, however, the saturated absorption line contains both phase and amplitude gratings that are related through a Kramers-Kronig relation. It is the combination of these two gratings that prevents the formation of noncausal echoes preceding the excitation pulses. A discussion of causality in photon-echo and spectral hole-burning is given by Saari *et al.*[23]. In this section, we describe an experiment that has all the features of an accumulated photon echo experiment: Echoes are generated at the expected time delay after the excitation pulse-pair, multiple echoes are observed for strong excitations, and the echo intensity decays as the separation between the excitation pulses is increased, suggesting a limiting homogeneous process. The striking difference between this experiment and a photon-echo experiment is that *echoes are generated symmetrically, both following and preceding the excitation pulses*, in what might appear as a violation of causality.

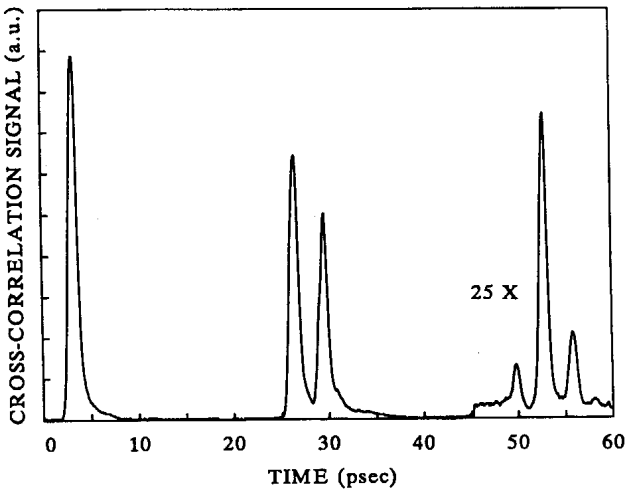

Figure 10. Experimental setup for generation of noncausal echoes. The nonlinear medium is a liquid solution producing thermally induced refractive-index changes.

The experimental setup is shown in Fig. 10. The main component is a nondispersive grating-and-lens system, commonly used for pulse shaping of ultrashort pulses[24,18]. The gratings had 1200 lines/mm, and the focal length of the lenses was 25 cm. The system is aligned so that it transmits short optical pulses without temporal distortions. A cell containing a nonlinear index material was then placed at the confocal plane of the system. The nonlinear element was a 1-mm-long

cell with an aqueous solution of copper sulfate that absorbed ~75% of the light and produced thermal changes in the refractive index.

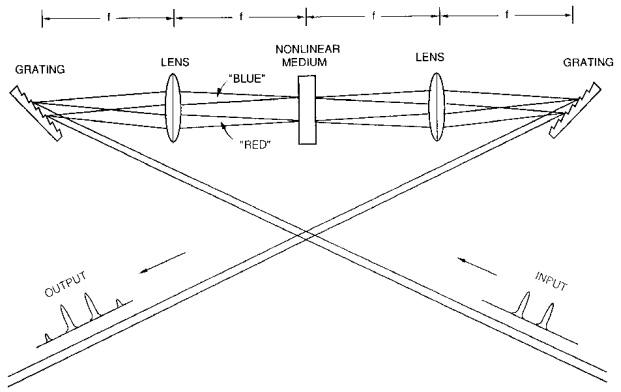

Figure 11. Time-resolved signal emerging from the system for three different delays between the input pulses: 0.4 ps (top), 0.8 ps (middle), and 1.3 ps (bottom). the first-order echoes are marked by arrows.

The input signal in the experiment was a sequence of pulse pairs derived from a mode-locked Ti:sapphire laser system at a rate of 82 MHz. Each pulse was ~80 fs in duration, and the separation between the pulse pair was varied by adjusting the relative delay between the arms of a Michelson interferometer. The signal emerging from the system was cross-correlated with a single short pulse through second-harmonic generation. Fig. 11 shows the cross-correlation signals obtained for three different delays between the input pulses. The two input pulses are preceded and followed by new echo pulses. Note the symmetric echo generation, the higher-order echoes, and the decay of the echo with increasing delay.

To understand this result, remember that the two closely spaced pulses interfere to generate a sinusoidally modulated spectrum. If $A(\omega)$ is the spectrum of a single pulse, a pair of equal-amplitude pulses separated by τ is characterized, up to a phase term, by

$$S_i(\omega) = 2A(\omega)\cos(\omega\tau/2). \tag{2}$$

This spectrum is dispersed in space inside the nonlinear medium, and each frequency component acquires nonlinear phase shift $\phi_{\rm nl}$ proportional to its intensity. This results in a distorted spectrum,

$$S_f(\omega) = S_i(\omega)\exp[i\phi_{\rm nl}(\omega)], \tag{3}$$

where

$$\phi_{\rm nl}(\omega) = \beta|S_i(\omega)|^2. \tag{4}$$

Here β is a coefficient that reflects the strength of the nonlinear interaction. The periodic spectrum is now distorted. When this spectrum is transformed back to the time domain, it leads to higher harmonics, or echoes. Because the distortion is a pure phase distortion (no change in transmission), the echoes are generated symmetrically around the input pulses.

This process is precisely analogous to the formation of photon echoes in an inhomogeneous absorber, where the sinusoidally modulated spectrum of the pulse pair saturated a frequency grating in the inhomogeneous line. There, however, the saturated absorption line results in a phase and amplitude gratings that are connected through a Kramers-Kronig relation, preventing the formation of noncausal echoes preceding the excitation pulses. In our nonlinear pulse shaper, because the frequencies are dispersed in space, the spectrum is affected by a pure phase grating, free of any amplitude modulation; hence we are not limited by the causal relation of the usual photon-echo process. We can conclude then that the echoes generated in this experiment and the photon-echo generated in inhomogeneous absorbers are completely analogous. Because our nonlinear material is much slower than the pulse repetition rate and the nonlinear index builds up over many pulse pairs, our experiment is equivalent to an accumulated photon-echo experiment[25].

In Eqs. (1)-(3), we assume that each frequency element affects only its own phase. In practice, there are two processes that change this ideal situation. First, the limited resolution of the optical system results in a finite spot size to each frequency element in the focal plane. In addition, thermal diffusion in the nonlinear medium may smear the index grating. If these processes are important, then to obtain the nonlinear phase shift, the spectrum should be convolved with an effective spectral impulse response function $H(\omega)$:

$$\phi(\omega) = \beta|S(\omega)|^2 * H(\omega), \tag{5}$$

where $*$ symbolizes the convolution operation. The consequence of Eq. (4) is a decrease in the efficiency of the formation of the spectral grating as τ is increased, and

as a result there is a decrease in the efficiency of the echo formation. In a standard photon-echo experiment, the decay of the echo as a function of the pulse delay τ is a convenient way of measuring the homogeneous width within an inhomogeneous line[27]. The decay is caused by the inability to saturate a frequency grating that is finer than the homogeneous linewidth. Here the decay is a measure of the width of the effective impulse response function $H(\omega)$. Fig. 12 shows the measured echo intensity as a function of the delay. The echo decay can be approximated by an exponential function $\exp(-4t/T_2^{\rm eq})$, with an equivalent homogeneous lifetime $T_2^{\rm eq} \approx 1.5$ ps. This lifetime is equivalent to an homogeneous width of 0.8 nm. Because the calculated spectral resolution of the system is 0.15 nm, we attribute this width primarily to the washout of the thermal grating in our cell.

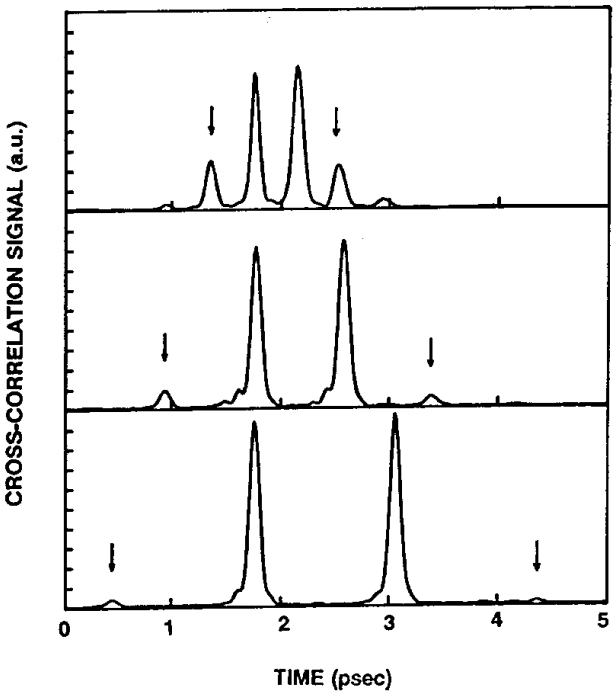

Figure 12. Decay of the echo as a function of the delay between the pulses. Circles (crosses) mark the preceding (following) echo pulse intensity. The solid line depicts exponential decay $\exp(-t/0.375)$.

What about the apparent violation of causality? Indeed, once the nonlinear material is introduced into the system, echoes are detected prior to the arrival of the excitation pulses. Still, there is nothing that violates causality. By spreading the spectral components in space, we indeed can perform linear and nonlinear filtering functions on the signal, and the filter function is not limited by a Kramers-Kronig-type relation. In particular, the signal energy can be shifted forward and backward in time. However, this shift is limited to a finite temporal window around the pulse. This window can be reproduced experimentally by placing a slit at the focal plane of the pulse-shaping system and sending a short pulse through the apparatus. As the slit is narrowed, the output pulse broadens in time owing to the narrower transmitted spectrum, and the broadening is symmetric around the pulse center[25]. However, once the slit is narrower than the spectral spot size, the signal does not broaden further but just attenuates. This broadest pulse defines the temporal window of the system, and it was measured to be $\sim$4 ps (FWHM) in our setup. It can be shown that the temporal extent of the window is determined only by the geometric relation between the beam and the gratings[24].

Nonlinear pulse shaping can be applied in signal processing of short temporal signal. Photon echo has been considered for similar applications, but it can be achieved only in inhomogeneous absorber at cryogenic temperatures. Our system can reproduce the same effects by using conventional third-order nonlinear materials, such as the thermal medium demonstrated here. A demonstration of some of these possibilities has been reported recently by Weiner *et al.*[28] in a system that used a permanent recording medium instead of a real-time nonlinear medium. Their experiment was referred to as spectral holography. A pulse-shaping system was used to demonstrate recording and subsequent readout of ultrashort signal in a holographic recording medium. Our experiment can be thought of as a real-time version of spectral holography.

VI. Conclusion

This paper reviewed accumulated photon-echo experiments in erbium-doped optical fibers. These experiments demonstrate the advantage of single-mode optical fibers for investigation of resonant coherent effects. We have also demonstrated the capability of ultrafast time-domain signal processing in doped fibers. The inhomogeneous width of the 1.53 μm transition we have investigated can support pulses as short as 0.5 ps. With the estimated $\sim$1 ns homogeneous dephasing

time, these fibers can handle (store or process) about 1000 bits at rates of 1 Tbit/s. We have not observed in our experiment long term effects due to persistent hole burning, which are known to be weaker in glasses as compared with crystalline hosts[29]. Without such effects, the storage time is determined by the ~10 ms relaxation time of the transition used. Note that these processes take place inside a fiber, at a wavelength that is central to optical communication systems, and where fiber-based amplifiers and lasers are now easily available.

We have also presented a frequency-domain analysis of the accumulated photon-echo process that is particularly suitable for the highly saturated, highly absorptive experiments in fibers. This simple and intuitive approach makes clear the origin of the causal nature of the photon-echo process. We also reported an experiment where the causal constraints are removed and echoes preceding the excitation pulse-pair are generated. In such an experiment, a grating pair pulse shaper which includes a third order nonlinear material is used, and ultrafast signal processing can be performed without the need of an inhomogeneous absorber at cryogenic temperatures.

References

1. See for example, G.P. Agrawal, *Nonlinear Fiber Optics*, Quantum Electronics - Principles and Applications Series. New York: Academic, 1989.
2. J. Hegarty, M.M. Broer, B. Golding, J.R. Simpson, and J.B. MacChesney, Phys. Rev. Lett. **51**, 2033 (1983); J. Hegarty, J. Lumin. **36**, 273 (1987).
3. V.L. da Silva, Y. Silberberg, J.P. Heritage, E.W. Chase, M.A. Saifi, and M.J. Andrejco, Opt. Lett. **16**, 1340 (1991).
4. V.L. da Silva and Y. Silberberg, Phys. Rev. Lett. **70**, 1097 (1993).
5. Y. Silberberg, V.L. da Silva, J.P. Heritage, E.G. Chase and M.J. Andrejco, IEEE J. Quantum Electron. **28**, 2369 (1992).
6. M. Nakazawa, Y. Kimura, K. Kurokawa, and K. Suzuki, Phys. Rev. A **45**, R23 (1992).
7. V.L. da Silva and Y. Silberberg, Opt. Lett. **18**, 580 (1993).
8. N.A. Kurnit, I.D. Abella, and S.R. Hartmann, Phys. Rev. Lett. **13**, 567 (1964); I.D. Abella, N.A. Kurnit, and S.R. Hartmann, Phys. Rev. **141**, 391 (1966).
9. T. Mossberg, Y. Flussberg, R. Kachru and S.R. Hartmann, Phys. Rev. Lett. **42**, 1665 (1979).
10. W.H. Hesselink and D.A. Wiersma, Phys. Rev. Lett. **52**, 1991 (1979).
11. W.H. Hesselink and D.A. Wiersma, J. Chem. Phys. **75**, 4192 (1981).
12. A. Schenzle, R.G. De Voe, and R.G. Brewer, Phys. Rev. A **30**, 1866 (1984).
13. A.K. Rebane, R.K. Kaarli, P.M. Saari, JETP Let. **38**, 383 (1983); A. Rebane, J. Aaviksoo, and J. Kuhl, Appl. Phys. Lett. **54**, 93 (1989).
14. E. Desurvire, J.L. Zyskind, and J.R. Simpson, IEEE Photon. Technol. Lett. **2**, 246 (1990); E. Desurvire and J.R. Simpson, Opt. Lett. **15**, 547 (1990).
15. See for example, E. Desurvire, *Erbium-Doped Fiber Amplifiers: Principles and Applications*, John Wiley & Sons Inc., New York (1994).
16. M.A. Saifi, M.J. Andrejco, W.I. Way, A. Von Lehman, A.Y. Yan, C.Lin, F. Bilodeau, and K.O. Hill, in Techn. Dig., Optical Fiber Commun. Conf. 1991, paper FA6, 198 (1991).
17. C.P. Yakymyshyn, J.F. Pinto, and C.R. Pollock, Opt. Lett. **14**, 621 (1989).
18. A.M. Weiner, J.P. Heritage, and E.M. Kirschner, J. Opt. Soc. Am. B **5**, 1563 (1988).
19. T.W. Mossberg, Opt. Lett. **7**, 77 (1982).
20. N.W. Carlson, L.J. Rothberg, A.G. Yodh, W.R. Babbit, and T. W. Mossberg, Opt. Lett. **8**, 483 (1983); N.W. Carlson, Y.S. Bai, W.R. Babbit, and T. W. Mossberg, Phys. Rev. A **30**, 1572 (1984); Y.S. Bai, W.R. Babbit, N.W. Carlson, and T. W. Mossberg, Appl. Phys. Lett. **45**, 714 (1994); W.R. Babbitt and T.W. Mossberg, Opt. Comm. **65**, 185 (1988).
21. M.K. Kim and R. Kachru, Opt. Lett. **12**, 593 (1987); M.L. Kim and R. Kachru, Opt. Lett. **14**, 423 (1989).
22. J.W. Goodman, *Introduction to Fourier Optics*, McGraw-Hill, New York (1968).
23. P. Saari, K. Kaarli, and A. Rebane, J. Opt. Soc. Am. B **3**, 527 (1986).

24. J.P. Heritage, A.M. Weiner, and R.N. Thurston, Opt. Lett. **10**, 609 (1985).
25. Note that every narrow filter will broaden a short pulse, but in most filters, such as Fabry-Perot-type interference filters, the temporal broadening is asymmetric and the signal is always delayed by the filter. In these filters, which are limited by a Kramers-Kronig relation, the signal is never pushed forward in time.
26. W.H. Hesselink and D.A. Wiersma, Phys. Rev. Lett. **43**, 1991 (1979).
27. L. Allen and J.H. Eberly, *Optical Resonance and Two-Level Atoms*, Wiley, New York (1975).
28. A.M. Weiner, D.E. Leaird, D.H. Reitze, and E.G. Paek, Opt. Lett. **17**, 224 (1992)
29. R.M. Macfarlane and R.M. Shelby, in *Spectroscopy of Solids Containing Rare Earth Ions*, A.A. Kaplyanskii and R.M. Macfarlane, Eds., Elsevier Science Publishers, pp. 51 (1987).